

# Magnetic and Optical Anisotropy in Garnets Induced by Linearly Polarized Light

**I.I. Davidenko,**

*Kiev Taras Shevchenko National University, UKRAINE,*  
[daviden@ukrpack.net](mailto:daviden@ukrpack.net)

**M. Fally and R. A. Rupp**

*Institute of Experimental Physics, Vienna University, Austria*  
[Martin.Fally@exp.univie.ac.at](mailto:Martin.Fally@exp.univie.ac.at), [Romano.Rupp@exp.univie.ac.at](mailto:Romano.Rupp@exp.univie.ac.at)

**B. Sugg**

*Robert Bosch GmbH, Stuttgart, Germany*

**Abstract:** A theoretical model is developed which clarifies the reason for the appearance of a magnetic and/or optical anisotropy in garnets under illumination with linearly polarized light. The model is based on the calculation of the occupancies' kinetics of anisotropic impurity centers localized in different garnet sublattices. A comparison of experimental data for the magnetic yttrium-iron garnet doped with cobalt (YIG:Co) and the non-magnetic  $\text{Ca}_3\text{Mn}_2\text{Ge}_3\text{O}_{12}$  (CaMnGe) garnet to the results of the model is performed which leads to a good agreement.

**OCIS codes:** (260.1440) Birefringence, (160.0160) Materials.

## Introduction

Currently photoinduced effects (PIE) are investigated in a wide class of magnetic and non-magnetic materials, such as garnets of different compositions [1,2,3], spin glasses [4], ferrites [5], cyanides [6], metals [7], etc. Magnetic and non-magnetic garnets usually were employed as model systems due to their well investigated magnetic and optical properties. PIE independent on the polarization state as well as all kinds of polarization-sensitive PIE have been observed in garnets. The recent discovery of PIE at room temperature [2] and the relative simplicity of forming magnetic or optical anisotropies under illumination with polarized light open a perspective to the practical use of PIE, e.g. for information storage and processing or for optoelectronic devices.

A general condition for the appearance of PIE in garnets is the presence of highly anisotropic light-sensitive impurity centers in the crystal lattice. In particular it is important that such anisotropic ionic centers can exist in states with different valencies. According to recent findings, the nature of the PIE is connected with an optical excitation of anisotropic impurity centers and their redistribution among non-equivalent sites, thus changing their fraction of occupancy. Such a redistribution among non-equivalent sites resulting from illumination with polarized light leads to macroscopic magnetic and/or optical anisotropies. In order to clarify the mechanism it is preferable to refrain from the complications which arise from magnetization and magnetic domain structure. In this paper we therefore consider manganese-germanium garnets (MnGeG) which are non-magnetic systems at room temperature. Cobalt substituted yttrium iron garnet (YIG:Co) is utilized as an example of a magnetic medium.

The aim of the present work is to develop a theoretical model to explain the formation of an optical anisotropy in MnGeG and a magnetic anisotropy in YIG:Co under the influence of linearly polarized light. From an experimental point of view the optical anisotropy reveals itself as a photoinduced linear birefringence

(PLB)  $\Delta n_{\text{PLB}}$ . The appearance of a light induced magnetic anisotropy (LIA) is the reason for the experimentally observed [1,2] photoinduced magnetization switching in magnetic garnets. The simple theoretical model to be developed below can be generalized easily to explain PIE in other media with photoactive anisotropic impurity centers. The approach used here is rather general in the sense that it is not necessary to know the particular nature and the properties of impurity centers which are responsible for the PIE .

## Model

Following the idea of *Gnatchenko et al.* [8] we assume that the appearance of linear birefringence in CaMnGeG under the influence of polarized light can be attributed to the redistribution of the  $\text{Mn}^{3+}$  ion occupancies between the octahedral sites of the crystal lattice. Redistribution of  $\text{Mn}^{3+}$  is possible due to presence of  $\text{Mn}^{4+}$  which can be considered as Mn-holes [9] serving as the centers of charge transfer. The ground state  ${}^4A_{2g}$  of  $\text{Mn}^{4+}$  has no orbital degeneracy and therefore does not create any distortions of the oxygen environment. Without the influence of polarized light  $\text{Mn}^{4+}$  ions are distributed uniformly among different octahedral positions. In an octahedral oxygen environment the energetic ground state  ${}^5E_g$  of  $\text{Mn}^{3+}$  is threefold degenerate. Therefore these ions produce a trigonal distortion of the octahedral oxygen environment, thus reducing the site symmetry. The nonuniform distribution of the  $\text{Mn}^{3+}$  among different octahedral positions results in the appearance of inhomogeneous strains and hence to an optical anisotropy.

In the magnetic YIG:Co the  $\text{Co}^{2+}$  ions are considered as the photoactive centers which are responsible for the magnetic PIE. The optical recharge of  $\text{Co}^{2+}$  in octahedral sites of YIG:Co accomplishes through the conduction band formed by overlapping 3d-orbits of the iron ions [2,10]. By absorbing a light quantum the  $\text{Co}^{2+}$  in the octahedral sites are excited delivering a photoelectron to the conduction band. After its finite life time the electron is captured by  $\text{Co}^{3+}$  in another octahedral site, i.e. effectively a transfer  $\text{Co}^{2+} \leftrightarrow \text{Co}^{3+}$  occurs. Optical recharge of tetrahedral cobalt ions happens in the same way, however, those ions make a considerably smaller contribution to the magnetic anisotropy [11] and are not taken into account in the present consideration.

The symmetry of the garnet remains still 4/m, thus four differently oriented sites of the trigonal Wykoff symmetry occur. The trigonal axis is one of the principal axes of the electric dipole moment. If a light quantum is absorbed by the octahedral  $\text{Mn}^{3+}$  or  $\text{Co}^{2+}$  ions, the probability for a photoexcitation of the ion depends on the angle between the dipole moment of electron transition and the light polarization vector. On the other hand, the direction of dipole moment of electron transition is hardly connected with the electric dipole moment in the initial state, i.e. with the orientation of the local trigonal axis. Thus, the probability of a photoexcitation of the active centers is different for different octahedral sites.

In what follows we consider the absorption of linearly polarized light propagating in the [001] direction. We assume that the light quantum is absorbed by a  $\text{Mn}^{3+}$  ion (or  $\text{Co}^{2+}$ ), which is located in an octahedral site with its local anisotropy axis directed along one of the crystallographic directions  $\langle 111 \rangle_i$  ( $i=1,2,3,4$ ). By the absorption of light an electron transition from the initial state  $S_1$  into the final state  $S_2$  occurs. At the present stage it is not necessary to concretize the nature of the states  $S_1$  and  $S_2$ . However, it is straightforward to suppose, that  $S_1$  is the ground state of the ion  $\text{Mn}^{3+}$  (or  $\text{Co}^{2+}$ ) in an octahedral site with the direction of the dipole moment along the local trigonal axes  $\langle 111 \rangle_i$ . Neglecting the finite life time in an excited state the probability of photoabsorption per unit of time  $\nu_i$  of the ion in the dipole approximation can be expressed by:

$$\tilde{\sigma}_i = \frac{2\pi^2}{\hbar c} \left[ \langle S_2 | (\vec{e}_{\parallel} \cdot \vec{d}_i) | S_1 \rangle^2 \delta(f_{12} - f) + \langle S_2 | (\vec{e}_{\perp} \cdot \vec{d}_i) | S_1 \rangle^2 \delta(f_{12} - f) \right] \quad (1)$$

where  $\bar{e}_{\parallel}$  and  $\bar{e}_{\perp}$  are the components of the light polarization coordinate vector of the incident light along and perpendicular to  $\langle 111 \rangle_i$  direction, respectively.  $\bar{d} = -e\bar{r}$  is the dipole moment of the electron transition, and  $\langle S_2 | (\bar{e}_{\parallel} \cdot \bar{d}_i) | S_1 \rangle^2$  and  $\langle S_2 | (\bar{e}_{\perp} \cdot \bar{d}_i) | S_1 \rangle^2$  are the matrix elements of the dipole moment of the electron transition from the state  $S_1$  into the state  $S_2$  with the corresponding frequency  $f_{12}$ . Eq. (1) can be rewritten to

$$\tilde{\omega}_i = \frac{2\pi^2}{\hbar c} e^2 I \left[ \langle S_2 | (\cos \psi_i \hat{e} \cdot \bar{r}_i) | S_1 \rangle^2 + \langle S_2 | (\sin \psi_i \hat{e} \cdot \bar{r}_i) | S_1 \rangle^2 \right] \quad (2)$$

where  $\hat{e}$  is the unit vector of the light polarization,  $I$  is the light intensity,  $\bar{r}_i$  is the radius-vector of the considered electron transition and  $\psi_i$  is the angle between light polarization vector and the local symmetry axes  $\langle 111 \rangle_i$ . If we introduce another notation for the matrix elements of radius-vector  $r_{i\perp} = \langle S_2 | r_{\perp} | S_1 \rangle$  and  $r_{i\parallel} = \langle S_2 | r_{\parallel} | S_1 \rangle$ , then Eq. (2) reads

$$\tilde{\omega}_i = \frac{2\pi^2}{\hbar c} e^2 I r_{i\perp}^2 \left( 1 + \frac{r_{i\parallel}^2 - r_{i\perp}^2}{r_{i\perp}^2} \cos^2 \psi_i \right) = A(1 + B \cos^2 \psi_i) \quad (3)$$

where  $A = \frac{2\pi^2}{\hbar c} e^2 I r_{i\perp}^2$  and  $B = \frac{r_{i\parallel}^2 - r_{i\perp}^2}{r_{i\perp}^2}$ .

Expression (2) is similar to that obtained in [12] for investigations of photoinduced dichroism in an yttrium-iron garnet doped with silicon.  $A$  and  $B$  are phenomenological constants which depend on the chemical composition of the garnet, the temperature, and the wavelength of incident light. It should be remarked that in the presence of magnetic order another term appears in (3) which depends on the angle  $\varphi_i$  between the  $\langle 111 \rangle_i$  direction and the vector of magnetization [12]:

$$\nu_i = A I (1 + B \cos^2 \psi_i) (1 + C \cos^2 \varphi_i) \quad (4)$$

where  $C$  is again a phenomenological constant.

Using Eq. (3) (or Eq. (4) for the magnetic case) it is possible to derive general expressions for the transition rate (velocity of the probability) of an electron to be excited from an octahedral center  $Mn^{3+}$  (or  $Co^{2+}$ ) under the absorption of a quantum of linearly polarized light. Accounting for the finite probability  $K$  of an electron excitation from an excited state of the ion and the thermoactivated transitions in the simplest way [13] leads to

$$\omega_i = A I K (1 + B \cos^2 \psi_i) + \nu \exp[-\epsilon_a / k_B T] \quad (5a)$$

$$\omega_i = A I K (1 + B \cos^2 \psi_i) (1 + C \cos^2 \varphi_i) + \nu \exp[-\epsilon_a / k_B T] \quad (5b)$$

for the  $MnGeG$  and the  $YIG:Co$ , respectively.

The second terms in Eqs. (5a) and (5b) describe the thermoactivated transitions, with  $\nu$  and  $\epsilon_a$  being their frequency factors and activation energies, respectively,  $k_B$  the Boltzmann constant, and  $T$  the temperature.

In the absence of light ( $I=0$ ) the first terms in Eqs. (5a) and (5b) vanish, and only a thermoactivated stimulation of an electron from the photoactive center is possible.

As a next step we include the particular symmetry of the garnet. It turns out that the transition rates for the stimulation (excitation) of an electron from photoactive centers under light illumination are different only for two among the four octahedral sites for MnGeG, and only for three octahedral sites for YIG:Co, respectively. To study the redistribution of the occupancies  $n_i$  in the octahedral centers under light illumination a system of kinetic equations is set up:

$$\frac{dn_i}{dt} = -\omega_i n_i + \frac{1}{3} \sum_{i \neq j, i=1}^3 \omega_j n_j \quad \sum_{i=1}^3 n_i = N \quad (6)$$

Evidently, Eq. (6) consists of 3 equations for YIG:Co (magnetic state) and of only 2 equations for MnGeG (non-magnetic state) and can be easily solved analytically.

Here, we consider the simplest case of the non-magnetic state of MnGeG in detail. The initial conditions for the system Eq. (6) are naturally obtained by assuming equal octahedral occupancies prior to the illumination, hence:  $n_1|_{t=0} = n_2|_{t=0} = N/2$ .  $N$  is the total concentration of photoactive impurity centers in octahedral sites. The solutions of the system of linear differential Eqs. (6) describe the time dependence of the occupancies of two different octahedral photoactive impurity centers under irradiation with linearly polarized light.

For a comparison of the model with experimental data [8] we assume that the value of photoinduced birefringence  $\Delta n_{PLB}$  is proportional to the difference of those occupancies  $\delta n = n_1 - n_2$ . Solving the system Eq. (6) yields the time dependence of  $\delta n$  as a simple exponential form:

$$\delta n(t) = \delta n_s (1 - \exp[-t/\tau_1]) \quad (7)$$

where  $\delta n_s$  and  $\tau_1$  depend on the parameters appearing in Eq. (5a). Under illumination with linearly polarized light the saturation level  $\delta n_s$  is reached. By switching off the light a purely thermoactivated relaxation process will take place which is again governed by the system of Eqns. (6) with  $\omega_1 = \omega_2 = v \exp[-\epsilon_a/k_B T]$  and the initial conditions  $n_1|_{t=0} = n_{s1}$ ,  $n_2|_{t=0} = n_{s2}$ , where  $n_{s1}$  and  $n_{s2}$  are the occupancies  $n_1$  and  $n_2$  reached in the steady state after irradiation, i.e. in the saturation state. Similarly, the difference of occupancies in case of the pure relaxation process is:

$$\delta n(t) = \delta n_s \exp[-t/\tau_0] \quad (8)$$

where  $\delta n_s = n_{s1} - n_{s2}$ ,  $\tau_0 = 1/2\omega_0 = (2v \exp[-\epsilon_a/k_B T])^{-1}$ .

Analogous considerations for the magnetic case lead to the following expressions:

$$\begin{aligned} n_3 &= a_1 \exp[\lambda_1 t] + b_1 \exp[\lambda_2 t] + c_1 \\ n_2 &= a_2 \exp[\lambda_1 t] + b_2 \exp[\lambda_2 t] + c_2 \\ n_1 &= n_4 = \frac{1}{2}(N - n_1 - n_2) \end{aligned} \quad (9)$$

where  $\lambda_i$ ,  $a_i$ ,  $b_i$  and  $c_i$  are functions of  $N$  and  $\omega_i$ .

## Comparison with the experimental results

The experimentally measured parameters for non-magnetic and magnetic states were photoinduced linear birefringence (PLB) and effective field of LIA, respectively. These values were calculated within the framework of developed model to compare with experimental results.

### 1. Non-magnetic CaMnGe

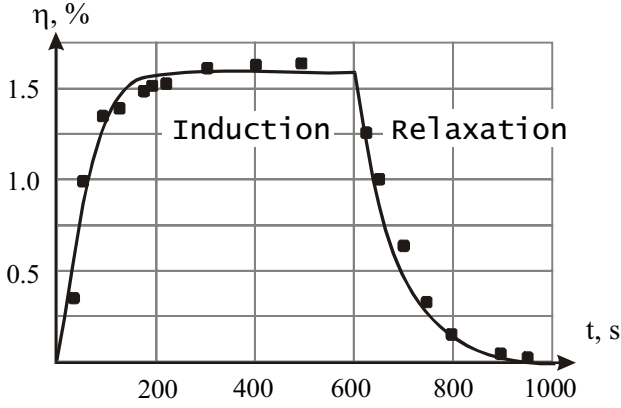


Fig. 1. Kinetics of PLB: Induction (recording) and relaxation (erasing).

(“Relaxation”) was obtained by illuminating the sample with circularly polarized light.

In general, the diffraction efficiency  $\eta$  for a refractive index grating (as in our case) at the exact Bragg condition is:

$$\eta = \sin^2 \left( \frac{\pi \Delta n d}{\lambda \cos \theta_m} \right) \quad (10)$$

Here  $d$  is the thickness of the grating,  $\lambda$  the wavelength of light,  $\theta_m$  is the Bragg angle in the medium and  $\Delta n$  the refractive index change. For a small argument in the  $\sin^2$ -function we approximate  $\eta \sim (\Delta n)^2 = (\Delta n_{\text{PLB}})^2 \sim (\delta n)^2$ . Within the scope of the developed model we performed a fitting procedure on the experimental data shown in Fig. 1. The result is presented by solid lines in Fig. 1.

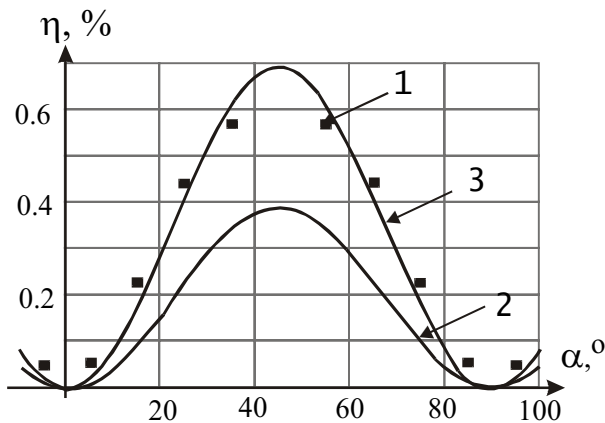


Fig. 2. Angular dependence of PLB

The experimental investigations on the kinetics - induction and relaxation - of PLB in CaMnGe garnet were reported in [8,14]. The measurements were performed on a thin (001)-plate of CaMnGe garnet in the paramagnetic phase at  $T=101\text{K}$ , considerably exceeding the Neel temperature ( $T_N = 13.85\text{K}$  [3]). A grating was recorded using two mutually orthogonal polarized light beams ( $\lambda=632.8\text{ nm}$ ) in a standard two wave mixing setup. The time dependence of the measured diffraction efficiency  $\eta$  is shown in Fig. 1 by solid squares. The grating results from the spatial dependence of PLB due to the spatially varying polarization of the “interfering” mutually orthogonal polarized light beams. The decay of  $\eta$  shown in Fig. 1

The decay of PLB under the influence of circularly polarized light can be described by an exponential law similar to Eq. (8) with a characteristic time constant  $\tau_2$ . The decay is not caused by temperature but by the influence of circularly polarized light.

It is also possible to calculate the dependence of the PLB on the angle  $\alpha = \angle(\vec{e}, \langle 111 \rangle)$  between the light polarization vector and the direction of the local anisotropy. The PLB in the saturation state as a function of that angle  $\alpha$  has been measured in Ref. [14] and is presented in Fig. 2 by solid squares. Solving Eq. (6)

with an angular dependent  $\nu_i$  and taking the limit  $t \rightarrow \infty$  yields PLB  $\Delta n(\alpha)$ . Using the fitting parameters obtained above the resulting curve is plotted in Fig. 2 (curve 2). The difference between the experimental data and the calculated values is due to the facts that the data presented in Fig. 1 and Fig. 2, respectively, were taken for different samples at different temperatures. Curve 3 in Fig. 2 shows the best fitting results for a free parameter  $\delta n_s$ .

## 2. Magnetic YIG:Co

The energy and the effective field of LIA were calculated for magnetic YIG:Co using Slonczewski's model [15] for a comparison with the experimental data:

$$W = -kT \sum_1^4 n_i \ln \left[ \cosh \left( \frac{3\alpha\lambda_o}{2k_B T} \cos \varphi_i \right) \right] - \frac{3\alpha^2\lambda_o^2}{4g\mu_B H_e} \sum_1^4 n_i \sin^2 \varphi_i \quad (11)$$

where  $\alpha\lambda_o$  and  $g\mu_B H_e$  are material parameters. The value of the effective field of LIA is  $H_L = W/M_s$ , where  $M_s$  is the saturation magnetization of the sample. Parameters obtained from the numerical fitting of the experimental results [16] were used for modeling.

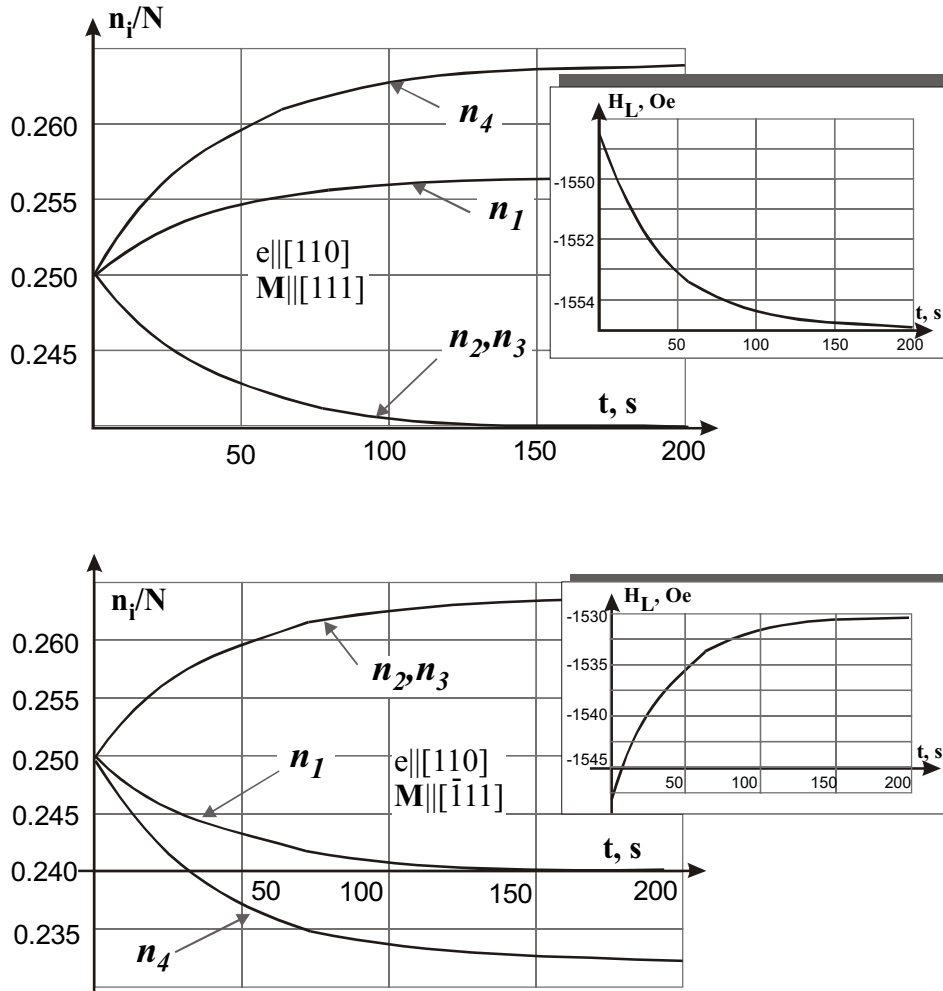


Fig. 3. Occupancies' kinetics of  $\text{Co}^{2+}$  ions in octahedral sites (YIG:Co) for two domains with different directions of magnetization

To compare the theoretical predictions with experimental results we accounted for the geometric configuration realized in the experiments for YIG:Co [2]. Linearly polarized light impinges on the sample along its crystallographic [001]-direction. A region including a boundary between two magnetic domains with magnetization directions  $\vec{M}||[111]$  and  $\vec{M}||[\bar{1}11]$ , respectively, was illuminated. The occupancies' kinetics of  $\text{Co}^{2+}$  in octahedral sites in these two magnetic domain states under illumination with linearly polarized light ( $\vec{e}||[110]$ ) were calculated for a homogeneous initial distribution of the occupancies. The kinetics and the changes of the effective field of LIA  $H_L$  - calculated from Eq. (11) - are shown in Fig. 3. It can be seen that  $H_L$  grows with time in one domain and decreases in the other. Thus, this is the reason for the experimentally observed effect of photoinduced spin reorientation [2].

## Conclusion

We have shown that for the non-magnetic state of a CaMnGe garnet the appearance of photoinduced linear birefringence can be attributed to the redistribution of occupancies between two types of octahedral centers forming two nonequivalent sublattices. Within the framework of a simple microscopic theoretical model the kinetics and angular dependencies of the PLB could be described. This is an improvement with respect to previous research [9,14], where these dependencies were estimated only at a phenomenological level from symmetry considerations. The good agreement between the experimental and theoretical results testifies the adequacy of the proposed theoretical approach to real physical processes.

We want to note, that a similar research was partly performed by the authors of Ref. [8]. They found, that experimentally that the kinetics of PLB cannot be precisely described by a simple exponential law. The non-exponential character of induction and relaxation of PLB may be caused by the existence of several independent channels of photoexcitation and relaxation with different characteristic times. The clarification of those features is subject of further studies.

In a further step we modified the approach to account for the magnetization in the magnetic garnet YIG:Co. Numerical simulation of the occupancies' kinetics of highly anisotropic  $\text{Co}^{2+}$  ions in octahedral sites of a YIG:Co garnet, as well as calculations of the effective field of LIA for the simplest conditions of illumination allow to explain the experimentally observed photoinduced magnetization switching.

Finally, we want to emphasize the universality of the theoretical model developed here. It does not require detailed information about the nature and peculiarities of photoactive anisotropic impurity centers as well as about the mechanisms of charge transfer between them. The model can be used for the explanation and description of photoinduced effects in any medium where orientation inequivalent crystal sites and charge transport between them are present.

## Acknowledgements

The work was supported by funds of the project INTAS 97-0366.

## References

1. V.F.Kovalenko and E.L.Nagaev, "Photoinduced magnetism", *Sov.Phys.Usp*, **29**, 297 (1986).
2. A.B.Chizhik, I.I.Davidenko, A.Maziewski and A.Stupakiewicz, "High-temperature photomagnetism in Co-doped yttrium iron garnet film", *Phys.Rev.B*, **57**, 22 (1998).
3. V.V.Eremenko, S.L.Gnatchenko, I.S.Kachur, V.G.Piryatinskaya, A.M.Ratner and V.V.Shapiro "Photoproduction and relaxation of long-lived active charges in  $\text{Ca}_3\text{Mn}_2\text{Ge}_3\text{O}_{12}$  garnet revealed through optical absorption", *Phys.Rev.B.*, **61**, 10670 (2000).
4. M.Ayadi and J.Ferre, "Photoinduced magnetic effects in an insulating spin-glass: cobalt aluminosilicate glass", *Phys.Rev.Lett.*, **50**, 274 (1983).

5. E.Katsnelson, "Photo-induced variation of optical and dielectric properties of ferrites at room temperature", *J.Appl.Phys.*, 77, 4604 (1995).
6. O.Sato, T.Iyoda, A.Fujishima and K.Hashimoto, "Photoinduced magnetization of a cobalt-iron cyanide", *Science*, 272, 704 (1996).
7. V.V.Afonin, V.L.Gurevich and R.Laiho, "Nonlinear photomagnetism of metals: theory of nonlinear photoinduced DC current", *Phys.Rev.B.*, 52, 2090 (1995).
8. V.A.Bedarev and S.L.Gnatchenko, "Photoinduction and relaxation of linear birefringence in manganese-germanium garnets", *Low Temp.Phys.*, 20, 124 (1994).
9. S.L.Gnatchenko, V.V.Eremenko, S.V.Sofroneev and N.F.Kharchenko, "Photoinduced linear birefringence in a crystal with cooperative ordering of Jahn-Teller distortions", *Sov. Pis'ma Zh. Exp. Teor.Fiz.*, 38, 198 (1983).
10. I.I.Davidenko, "Polarization sensitivity of photomagnetic effects in garnets", *OSA Trends in Optics and Photonics*, Volume XXVII, in *Advances in photorefractive materials, effects and devices*. 157 (1999).
11. M.D.Sturge, E.M.Gyorgy, R.C.LeCraw and J.P.Remeika, "Magnetic behavior of cobalt in garnets. Magnetocrystalline anisotropy and ferrimagnetic resonance in cobalt-doped yttrium iron garnet", *Phys.Rev.*, 180, 413 (1969).
12. J.F.B.Hawkes and R.W.Teale, "Spontaneous and photoinduced linear dichroism in silicon doped yttrium iron garnet", *J. Phys. C*, 5, 481 (1972).
13. R.P.Hunt, "Magnetic annealing effect in silicon-doped garnets", *J.Appl.Phys.*, 38, 2826 (1967).
14. Bertram Sugg. "Untersuchungen zu photorefraktiven Effekten bei tiefen Temperaturen", PhD Thesis, Shaker Verlag, Osnabrück, 1996 (in german).
15. J.C.Slonczewski, "Origin of magnetic anisotropy in cobalt-substituted magnetite", *Phys.Rev.*, 110, 1341 (1958).
16. In preparation.